The Different Aspects of Flexoelectricity in Nematics

J. P. Marcerou [a] & J. Prost [a]

[a] Centre de Recherche Paul Pascal, Domaine Universitaire, 33405, Talence, France
Version of record first published: 20 Apr 2011.

PLEASE SCROLL DOWN FOR ARTICLE

The Different Aspects of Flexoelectricity in Nematics†

J. P. MARCEROU and J. PROST

Centre de Recherche Paul Pascal, Domaine Universitaire, 33405 Talence, France

We report on an experimental investigation of the thermal dependence of the flexoelectric coefficient in the nematic phase of several compounds. It is found to vary essentially like the angular order parameter S. For the first time a symmetric compound (*pp'* hexyloxytolan) is shown to exhibit a "regular" flexoelectric behavior. All these observations are consistent with the quadrupolar interpretation, but we also define cases in which the dipolar contribution shows up.

Nous communiquons des résultats concernant la dépendance thermique du coefficient flexo-électrique dans la phase nématique de plusieurs composés. Nous trouvons qu'il varie essentielle-ment comme le paramètre d'ordre angulaire S. Nous montrons aussi, pour la première fois, qu'un composé symétrique (le *pp'* hexyloxytolane) a une activité flexoélectrique "normale". Ces observations sont compatibles avec l'interprétation quadrupolaire du phénomène, mais nous définissons aussi des cas dans lesquels il est possible de mettre en évidence la contribution dipolaire.

I INTRODUCTION

The flexoelectric effect describes the coupling of an electric field with the gradients of the director field in uniaxial media,[1] or equivalently the torque exerted by the electric field gradients on the director.[2] These alternative interpretations suggest two different microscopic approaches to the phenomenon. The original one, due to Meyer (and subsequently called the dipolar or the "Meyer" contribution) requires non-centrosymmetric (dipolar) molecules[1-7] (with the exception of Helfrich's remark on the induced asymmetry).[4] The second one takes into account the fact that the very symmetry of uniaxial phases leads to non-zero quadrupolar electric densities,[2] and is simply related to the interaction between an electric field

---

gradient and these quadrupolar densities. The fact that these two contributions might be of more or less equal importance may be seen just from dimensional arguments. The flexoelectric coefficient has the dimensions of a charge per unit length, that is in the dipolar picture a dipole moment of a typical nematic molecule over the square of its length[8] ($f \simeq$ a few 10^{-5} up to a few 10^{-4} esu cm^{-1}) and in the quadrupolar case a typical molecular quadrupole value times the number of particles per unit volume ($f \simeq$ a few 10^{-4} esu cm^{-1}).[2] Since these are just order of magnitude evaluations it is not possible to conclude really unambiguously as to whether one of the contributions is larger than the other. One needs a closer look and the answer can only be obtained if one is able to separate them out. The quadrupolar mechanism is best evidenced in the isotropic phase of nematogenic compounds.[9] On the other hand, an elegant way of measuring Meyer's contribution in the nematic phase consists in evidencing a relaxation of the flexoelectric coefficient $f = f_{\parallel} + f_{\perp}$ ($e_{1z} + e_{3x}$ in Meyer's notation) simultaneous to that of the longitudinal dipoles.[10] Unfortunately, for most compounds this last way of proceeding is not adapted. However, one is still able, in principle, to separate the two mechanisms out through the study of the thermal dependence of f. Indeed, the dipolar contribution is found to be essentially† proportional to the square of the nematic order parameter $S^{2,3,5}$ whereas the quadrupolar one should be simply proportional to S.[2] (For the definition of S see for instance Ref. 11).

Our "interdigital electrodes technique" is in principle well suited for such a study: as in any light scattering technique temperature control is easily achieved, and the flexoelectric phenomenon is naturally isolated (in the linear response regime) via the angular selection of the scattering geometry.[8] In fact, the situation is a little more involved and a more detailed analysis than the one given in Ref. 8 has to be performed before being able to interpret the experimental data. Most of the complications are closely related to the nature of the nematic phase and do not exist in either the smectic or the isotropic phases. One of the characteristics of the interdigital electrodes technique (Figure 1a–b) is to make use of a periodic inhomogeneous electric field, in order to induce a (periodic) tilt of the director. The geometry of the experiment is basically two dimensional, and its interpretation involves six unknowns (the director tilt δn_x (Figure 1b), the electric potential ϕ, the electric

---

† The calculation of Meyer's flexoelectric coefficient requires some statistical analysis. The S^2 dependence obtained in references[2,3,5] comes from the propagation of the molecular asymmetries by "long range" elastic forces; on the other hand, Straley's approach which deals with the short range distribution function, gives a dependence involving both S and S^2, however order of magnitude considerations based on formula (23) of Ref.[7] lead to estimates of f in the 10^{-6} range, which strongly suggest that the short range contribution is negligible compared to experimental values.

charge ρ^e, the velocity fields v_x, v_z and the hydrostatic pressure p (the nematic is assumed to be uncompressible). The usual laws of conservation, of hydro-dynamics (see Refs. 11, 12 and 13) and of electrostatics provide six coupled differential equations, which in the linear regime lead to a unique solution provided proper boundary conditions are satisfied. Such a solution is rather tedious and its use clumsy, so that it is desirable to make a number of approxi-mations which render the utilization of the technique easier. In the first description by Prost and Pershan[8] the simplest solutions, allowing for a sound physical description were used. In the second section of this paper we discuss their validity. In particular, the magnitude of the flexoelectric coefficient is such that in general the flexoelectric reaction field is not negligible and that one has to define the cases when such an approximation can be made (namely the importance of the reaction field is measured by the dimensionless parameter $4\Pi f^2/\varepsilon K$ in the elastic regime; with usual values of the dielectric constant $\varepsilon \simeq 5$, the Frank elastic constant $K \simeq 10^{-6}$ dyne, and anticipated values of $f \simeq 7 \cdot 10^{-4}$ esu cm^{-1} one gets a number of order unity, showing that one cannot ignore the reaction field (at low frequencies) without some special condition). The importance of boundary conditions will also be discussed, in connection with the frequency response of nematics.

In the third section, we give experimental results concerning the p,p'-methoxybenzilidene-n-butylaniline (MBBA), the p,p'-octyloxycyanobiphenyl (8OCB), the p,p'-dihexyloxytolan ("symmetric tolan") and the 4,n-pentyl-phenyl-4,(pentylbenzoyloxy)-3-chloro benzoate (3PBClB). The first three compounds have been chosen for the variable strength of their longitudinal dipole. Together with the temperature and the frequency dependences of the flexoelectric signal we discuss the anchoring conditions which seem to prevail in these experiments. When possible, we estimate the value of the flexoelectric coefficient f. The fourth compound is chosen for the very low relaxation frequency of its longitudinal dipole. As stressed before, and in Ref. 9 this allows the direct measurement of Meyer's contribution to flexo-electricity.

Eventually, in the fourth section we draw what we think to be the main conclusions of this study.

II THE TECHNIQUE

I Formulation of the problem

The basic features of the experiment are summarized on Figure 1a, b. Interdigital electrodes provide an electric field which is periodic in the x direction, and essentially contained in the zx plane (the extent of the stripes in the y direction is much larger than the period of the electric field $\lambda_e = 2\Pi/q_x$).
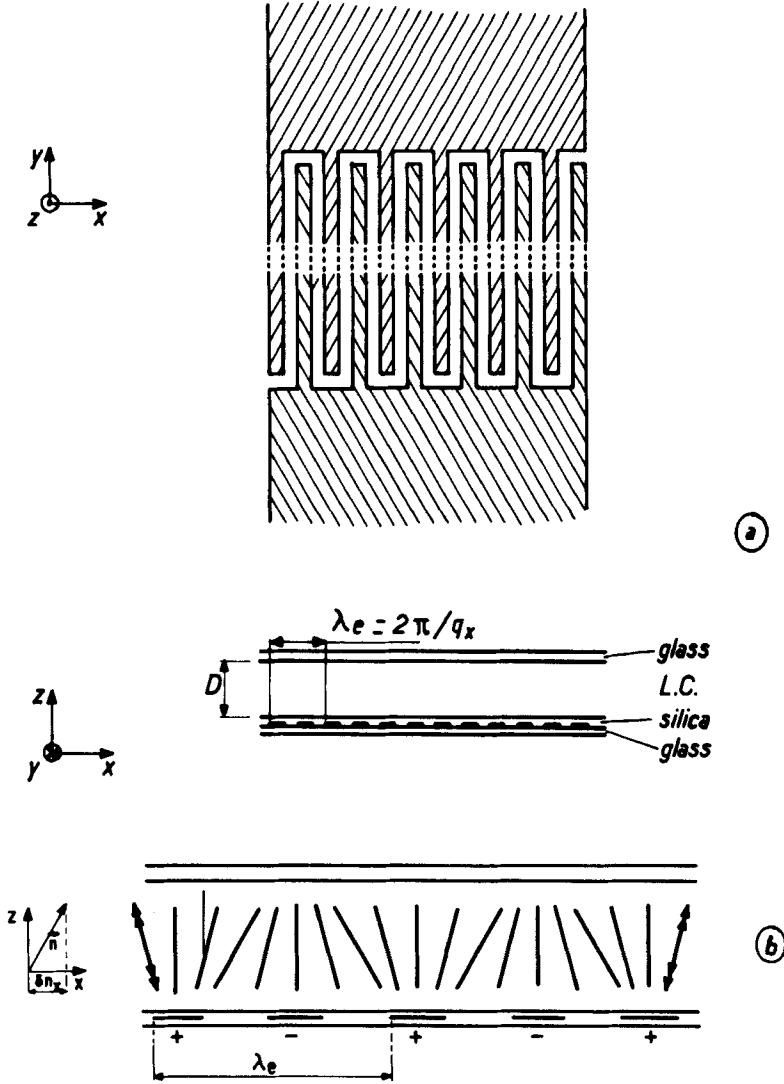
FIGURE 1   (a) Interdigital electrodes top and side views. The hatched areas represent a metal deposit (e.g.: Aluminium) on a glass substrate. The side view evidences a silicon dioxide layer which covers the metal, and protects the liquid crystal from a direct contact with the electrodes (typically 5000 Å thick). The gap of thickness D, comprised between the two glass slides is filled with a monocrystalline homeotropic liquid crystal, in typical experiments. The choice of the system axes is clear on the figure, and will be used throughout the paper. $\lambda_e = 2\pi/q_x$ is the period of the electric field. (Typically: $\lambda_e \simeq 5\mu m$, $D \simeq 500\mu m$). (b) Schematic representation of the distortion induced by a linear coupling of the nematic optical axis (or director) with the electric field generated by the electrodes. As usual the hydrodynamic variable δn_x, is the tilt angle of the director, away from its unperturbed direction z.
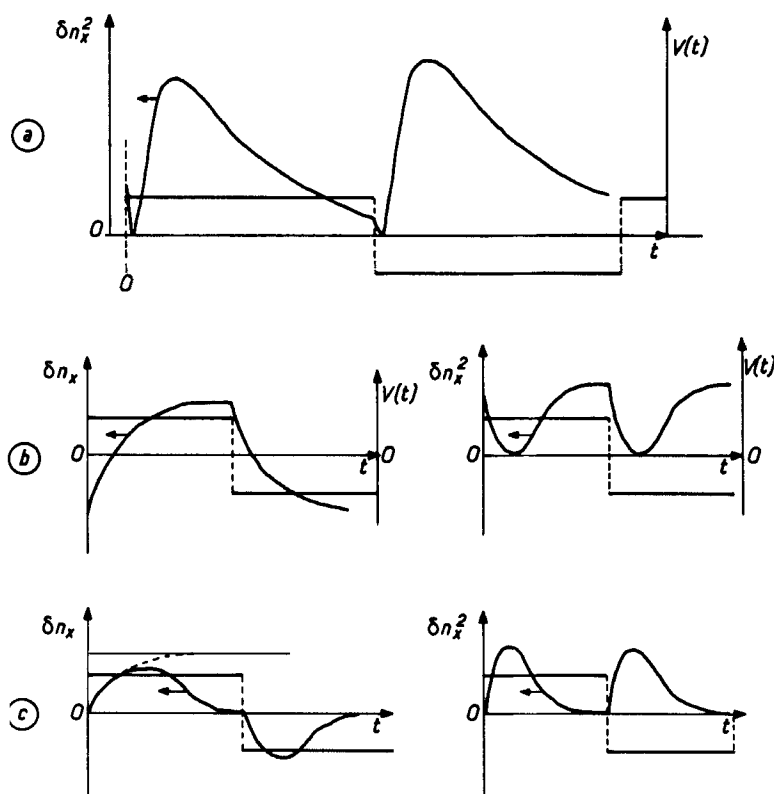
FIGURE 2 Cancellation of the flexoelectric signal through the screening of the applied electric field by space charges: (a) typical experimental homodyne response to a square wave potential of large period $T = 0.5$ sec. (MBBA at room temperature; applied voltage 0.5 volt). Note that the period is slightly too short to get complete cancellation of the signal but that the extrapolated behavior clearly goes to zero. (b) typical theoretical response in the absence of screening. (Left: heterodyning conditions; right: homodyning). (c) the screening effect; the signal does not reach the steady state limit, and is cancelled after a time characteristic of the charge motion (theoretical curve in which a single time constant for the charges is assumed). (Left: heterodyning condition; right homodyning conditions). Note the close similarity with the experimental curve. (For compounds like 8OCB, the steady state limit is reached before the screening takes place).

They are covered with an insulating SiO_2 layer which prevents a direct contact with the sample under study. The latter contained between the electrodes and a coverslide, has to be monocrystalline. In the following we used the homeotropic geometry (unperturbed optical axis or director n_0 along z so that the coupling of the field with the director induces a tilt $\delta n_x(x, z)$. The conditions under which the linear part of this coupling is singled out are explained in Ref. 8. The optical frequency dielectric tensor $\varepsilon_{ij}(x, z)$ is modulated

by the director tilt $\delta n_x(x, z)$, at spatial frequencies which are characteristic of the field distribution and coupling laws with the nematic axis. Optical scattering selection rules allow to single out the Fourier component $\delta\varepsilon_{ij}(q_x, q_z)$ proportional to the Fourier component $\delta n_x(q_x, q_z)$ which in the linear response regime, is non-zero only to the extent that a linear coupling with the electric field exists. As we will later see, it is important to check experimentally that one is really working within this linear regime.

The next point concerns the role of charges. When they have time to move, they screen out the applied electric field and no flexoelectric signal is observed in Ref. 8 and Figure 2. In the following calculations, we will assume that the temporal frequency of the field is such that they cannot move, and that they obey neutrality requirements of nematic $\rho^e = 0$. Such a domain exists with compounds like 8OCB, the symmetric tolan or 3 PBClB. We are thus left with a set of five variables, coupled by five linear differential equations (in the linear response limit):

$$\delta n(x, z, t) \quad \Phi(x, z, t), \quad p(x, z, t), \quad v_x(x, z, t) \quad \text{and} \quad v_z(x, z, t).$$

Deriving their expressions from the general hydrodynamic equations[12,13] is a standard exercise. As explained in Ref. 8, in the linear response limit the different Fourier components of the variables are uncoupled in the x direction. Furthermore a voltage sinusoidal in time is applied to the electrodes, so that we need only to consider time dependences of the type $e^{j\omega t}$. This allows to focus our attention on the equations for $\delta n(q_x, z, \omega)$, $(\partial/\partial t = j\omega$; $\partial/\partial x = jq_x)$ and ignore quadratic couplings which are linked to $\delta n(2q_x, z, 2\omega)$ or $\delta n(0, z, 0)$, $\delta n(2q_x, z, 0)$, $\delta n(0, z, 2\omega)$. One gets, in the Harvard's notations[12] (where for concision we introduce the molecular field[11] $h_x = -K_{11}q_x^2 \delta n_x + K_{33}(\partial^2/\partial z^2)\delta n_x + jf q_x(\partial/\partial z)\Phi$ and δn_x stands for $\delta n_x(q_x, z, \omega)$ and so on).

$$
\begin{bmatrix}
-K_{11}q_x^2 + K_{33}\dfrac{\partial^2}{\partial z^2} & -1 & jfq_x\dfrac{\partial}{\partial z} & 0 & 0 & 0 \\[2ex]
4\Pi jf\dfrac{\partial}{\partial z} & 0 & \varepsilon_\perp^0 q_x^2 - \varepsilon_\parallel^0\dfrac{\partial^2}{\partial z^2} & 0 & 0 & 0 \\[2ex]
-j\omega & \dfrac{1}{\gamma_1} & 0 & \dfrac{1}{2}(\lambda + 1)\dfrac{\partial}{\partial z} & \dfrac{j}{2}(\lambda - 1)q_x & 0 \\[2ex]
0 & 0 & 0 & jq_x & \dfrac{\partial}{\partial z} & 0 \\[2ex]
0 & -\dfrac{1}{2}(\lambda + 1)\dfrac{\partial}{\partial z} & 0 & v_3\dfrac{\partial^2}{\partial z^2} - 2q_2 q_x^2 & jv_3 q_x\dfrac{\partial}{\partial z} & -jq_x \\[2ex]
0 & -\dfrac{j}{2}(\lambda - 1)q_x & 0 & jv_3 q_x\dfrac{\partial}{\partial z} & 2v_1\dfrac{\partial^2}{\partial z^2} - v_3 q_x^2 & -\dfrac{\partial}{\partial z}
\end{bmatrix}
\begin{bmatrix}
\delta n_x \\[2ex] h_x \\[2ex] \Phi \\[2ex] v_x \\[2ex] v_z \\[2ex] p
\end{bmatrix}
= \begin{bmatrix} 0 \end{bmatrix}
$$

$$\text{(II.1)}$$

K_{11}, K_{33} are respectively the Frank Oseen splay and bend elastic constants, $f = f_\parallel + f_\perp$ is the flexoelectric coefficient, $\lambda = -(\gamma_2/\gamma_1)$ a thermodynamic coefficient discussed in[12] the v_i shear viscosities, γ_1 the twist viscosity and $\varepsilon_\perp^0(\varepsilon_\parallel^0)$ the dielectric constant perpendicular to the director (parallel) at the frequency $\omega/2\Pi$. The first line of the matrix expresses the definition of the molecular field, the second the electrical neutrality of nematics under the afore mentioned assumption, the third the hydrodynamic equation for the director, the fourth the mass conservation law, the fifth and sixth the momentum conservation law in which inertial terms have been neglected.

The general solution for such a system of coupled differential equations has the form:

$$\delta n_x(q_x, z, \omega) = \sum_{i=1}^{8} n_x^i(q_x, \omega)e^{-q_i(q_x, \omega)z}$$

(and similar expressions for the other variables);

the calculation of the q_i's is standard, and leads to an eighth order algebraic equation. (It merely consists in replacing $\partial/\partial z$ by $-q_i$, and set the determinant of the matrix to zero). Eight arbitrary parameters (for instance the n^i's) are left in the general case. The solution corresponding to the interdigital technique, is determined from four pairs of boundary conditions at the surfaces $z = 0$ and $z = D$.

i) the director boundary conditions are obtained from the minimization of the surface free energy[8] keeping track of the contribution from bulk terms:

$$A\delta n_x - K_{33}\frac{\partial \delta n_x}{\partial z} - pE_x = 0 \qquad z = 0 \qquad (II.3)$$

$$A\delta n_x + K_{33}\frac{\partial \delta n_x}{\partial z} + pE_x = 0 \qquad z = D \qquad (II.4)$$

A is the anchoring energy[11] and p the surface polarization per unit area. That such a surface polarization might exist results from the vectorial symmetry of any interface and has been discussed in Ref. 8; it has further been used to explain discrepancies between different experiments performed with homogeneous electric fields[14] and their presence at free surfaces is thought to be able to drive surface phase transitions.[15]

Simple considerations show that, as the flexoelectric phenomenon, they lead to a linear coupling between the electric and the director fields: thus they may contribute to a non zero $\delta n_x(q_x, z, \omega)$ and one has to find a way of separating out this polarization from the flexoelectric effect.

ii) the electric potential value is fixed on the electrodes and continuous at other interfaces.

iii) the velocities v_x and v_z have to vanish the $z = 0$ and $z = D$ planes. These last conditions which were not specifically included in Ref. 8, lead to sizable complications in the expression of the results. It turns out, that in the experimental section we are able to show that the correction brought about by the fulfilment of these last boundary conditions, is negligible for MBBA; it is impossible however, to generalize this statement to any nematic.

All these considerations show evidently that a systematic use of this technique is slightly compatible with such a lengthy treatment. One has to look for limiting cases in which simplifications can safely be made. Firstly, although not obvious in the matrix structure, the determinantal equation involves q_i^2 rather than q_i. This implies that four roots have a positive real part and four a negative one. If one chooses the thickness of the sample such that $(\text{Re}\{q_i\})$. $D \gg 1$, which is always satisfied if $q_x D \gg 1$, one can ignore boundary conditions in the plane $z = D$ and keep only those values of the q_i's which have a positive real part. Even with this last restriction, the problem is not quite easily tractable. One can however find closed solutions in two distinct limits:

—the elastic regime ($\omega \sim 0$); (its experimental existence depends on the comparison of the viscoelastic relaxation with the charged impurities characteristic frequencies);

—the viscous regime (frequency larger than any viscoelastic relaxation frequency).

II   The Elastic Regime

One finds the equations relevant to that case, by setting $\omega = v_x = v_z = 0$, in $|1|$ or $|2|$. The determinantal equation defines two wave vectors:

$$q_1^2 = \frac{q_x^2}{2}\left\{\frac{4\Pi f^2}{\varepsilon_\parallel^0 K_{33}} + \frac{\varepsilon_\perp^0}{\varepsilon_\parallel^0} + \frac{K_{11}}{K_{33}} + \sqrt{\left(\frac{4\Pi f^2}{\varepsilon_\parallel^0 K_{33}} + \frac{\varepsilon_\perp^0}{\varepsilon_\parallel^0} + \frac{K_{11}}{K_{33}}\right)^2 - 4\frac{\varepsilon_\perp^0}{\varepsilon_\parallel^0}\frac{K_{11}}{K_{33}}}\right\}$$

$$q_2^2 = \frac{q_x^2}{2}\left\{\frac{4\Pi f^2}{\varepsilon_\parallel^0 K_{33}} + \frac{\varepsilon_\perp^0}{\varepsilon_\parallel^0} + \frac{K_{11}}{K_{33}} - \sqrt{\left(\frac{4\Pi f^2}{\varepsilon_\parallel^0 K_{33}} + \frac{\varepsilon_\perp^0}{\varepsilon_\parallel^0} + \frac{K_{11}}{K_{33}}\right)^2 - 4\frac{\varepsilon_\perp^0}{\varepsilon_\parallel^0}\frac{K_{11}}{K_{33}}}\right\}$$

(II.5)

In the absence of flexoelectric coupling they correspond to the penetration of elastic deformations $(K_{11}/K_{33})q_x$ and of the electric field $(\varepsilon_\perp^0/\varepsilon_\parallel^0)q_x$. When $\varepsilon_\perp^0/\varepsilon_\parallel^0 > K_{11}/K_{33}$, the flexoelectric coupling tends to reduce the electric field penetration, but conversely the range of the elastic deformation is increased (the reverse occurs if $\varepsilon_\perp^0/\varepsilon_\parallel^0 < K_{11}/K_{33}$; note that this remark

which is not strictly correct since both $\delta n(z)$ and $\Phi(z)$ involve q_1 and q_2, is however meaningful to show the trend when the flexoelectric coupling is turned on.

Taking into account boundary conditions one finds:

$$\delta n_x(q_x, q_z \simeq 0) = \lim_{q_z \to 0} \int_0^D \delta n_x(q_x, z)\exp(jq_z z)dz$$

$$= -jq_x V_{q_x} \frac{(f + p)(q_1 + q_2) + fq_s}{(K_{11}q_x^2(q_1 + q_2) + q_s(K_{11}q_x^2 + K_{33}q_1q_2))} \quad \text{(II.6)}$$

($q_s = A/K$ is a measure of the anchoring strength as compared with q_x) ($V_{qx} = \Phi(q_x, z = 0, \omega = 0)$).

In the two limiting cases of strong ($q_s \gg q_x$) and weak ($q_s \ll q_x$) anchoring, one recovers the results given in Ref. 8:

Strong anchoring:

$$\delta n_x(q_x, q_z \simeq 0, \omega = 0) = -jV_{q_x} \frac{f}{K_{11}q_x + ((\varepsilon_\perp^0/\varepsilon_\parallel^0)K_{11}K_{33})^{1/2}q_x} \quad \text{(II.7)}$$

Weak anchoring:

$$\delta n_x(q_x, q_z \simeq 0, \omega = 0) = -jV_{q_x} \frac{f + p}{K_{11}q_x} \quad \text{(II.8)}$$

Remark

Such expressions do not represent closed solutions since one does not know a priori $V_{q_x} = \Phi(q_x, z = 0, \omega = 0)$. In Ref. 8 it was assumed that a good approximation was provided by the value obtained from the solution of Laplace's equation (under the condition $4\Pi f^2/\varepsilon K \ll 1$) that is $V_{q_x} \simeq V/2jG$ (V being the voltage directly applied on the electrodes and $G = F(1/\sqrt{2}, 1) \simeq 1.85$). This value is not likely to be grossly wrong since in any case $V/2$ and $-V/2$ are imposed on the electrodes' surfaces, and $\Phi(x, z = 0)$ has to be odd between two adjacent digits (Figure 3a, b). For instance, even in the case of Figure 3b, in which the dependence has been assumed markedly different from the Laplace's solution (Figure 3a) one finds $V_{q_x} \simeq (2\sqrt{2}/\pi^2 j)V$ the difference between the two values is only 6%. (This would of course be wrong for higher harmonics). The uncertainty introduced by using the first value is thus not expected to exceed 10%, and one may safely use Eqs. II.7, 8, with

$$V_{q_x} \simeq \frac{V}{2jG} \quad \text{(II.9)}$$
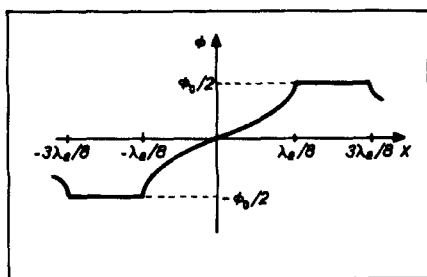
a .
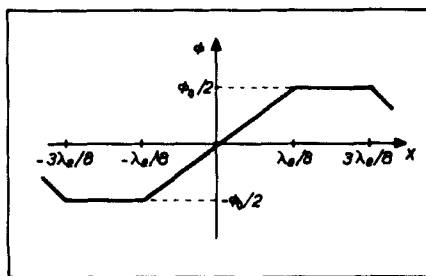
b .

FIGURE 3 $\phi(x, z = 0)$ as a function of x: (a) according to Laplace's equation (correct solution in the high frequency region). (b) trial function, that would be obtained if the corrections lead to a constant E_x field between the electrodes.

Inspection of these equations suggests two further remarks:

—if one wants to deal with flexoelectricity only, one has to realize experiments in the strong anchoring limit;

—the flexoelectric reaction field does not show up in the limit $q_z \simeq 0$, and the experiments will have also to take place in that range to avoid unneeded complications.

III   The high frequency (viscous) regime

When the frequency of the applied voltage increases, the amplitude of the induced director tilt decreases essentially like ω^{-1} above some characteristic viscoelastic frequency (typically $Kq_x^2/2\Pi\gamma_1$). The flexoelectric reaction field decreases in the same way, and the calculation of $\Phi(x, z)$ through the anisotropic Laplace's equation becomes correct. This limit is reached when

$4\Pi f^2 q_x^2/\varepsilon^0 \gamma_1 \ll \omega$. This also tells that one of the roots of the determinantal equation is $K^2 = (\varepsilon_\perp^0/\varepsilon_\parallel^0)q_x^2$. One is left with a sixth order algebraic equation for the other roots, namely:

$$\frac{-K_{11}q_x^2 + K_{33}q_i^2}{j\omega}\left(\frac{1}{\gamma_1^s} + \frac{\alpha}{\gamma_i}\frac{q_i^2}{q_x^2} + \frac{1}{\gamma_1^B}\frac{q_i^4}{q_x^4}\right) - \left(1 + \alpha\frac{q_i^2}{q_x^2} + \frac{q_i^4}{q_x^4}\right) = 0 \quad \text{(II.10)}$$

$$\left(\alpha = 2 \cdot \frac{v_3 - v_1 - v_2}{v_3}\right.$$

$$\frac{1}{\gamma_1^s} = \frac{1}{\gamma_1} + \frac{(\lambda - 1)^2}{4v_3} \qquad (\gamma_1^s = \text{splay viscosity})$$

$$\frac{1}{\gamma_1^B} = \frac{1}{\gamma_1} + \frac{(\lambda + 1)^2}{4v_3} \qquad (\gamma_1^B = \text{bent viscosity})$$

$$\left.\frac{1}{\gamma_i} = \frac{1}{\gamma_1} + \frac{\lambda^2 - 1}{2\alpha v_3}\right)$$

If one anticipates that one pair of solutions will grow like $\omega^{1/2}$, and the others be frequency independent, the factorization becomes obvious:

$$q_\omega^2 \simeq \frac{j\gamma_1^B \omega}{K_{33}}; \qquad q_{1,2}^2 \simeq \frac{q_x^2}{2}\left[-\alpha \pm \sqrt{\alpha^2 - 4}\right] \quad \text{(II.11)}$$

From that point on, solving for $\delta n_x, v_x$ or v_z, taking into account boundary conditions, is a straightforward algebraic exercise. The general expressions are rather bulky and we will simply give the solutions for $\delta n_x(q_x, q_z \simeq 0, \omega)$ in the weak and strong anchoring limits. One has however to first point out that these limits cannot be defined with respect to q_x as in the static case, but with respect to q_ω. If weak anchoring conditions are met in the elastic regime, they are a fortiori satisfied in the viscous regime ($q_s \ll q_x \ll q_\omega$) but the reverse is not true. Starting from strong anchoring conditions at low frequencies one always winds up in the weak anchoring limit provided one increases the frequency enough ($q_x \ll q_s \ll q_\omega$ or $\omega \gg A^2/K_{33}\gamma_1$); a "strong anchoring" viscous regime however exists within the range: ($q_x \ll q_\omega \ll q_s$ (Figure 4)).

—*Weak Anchoring*: ($q_s \ll q_\omega$)

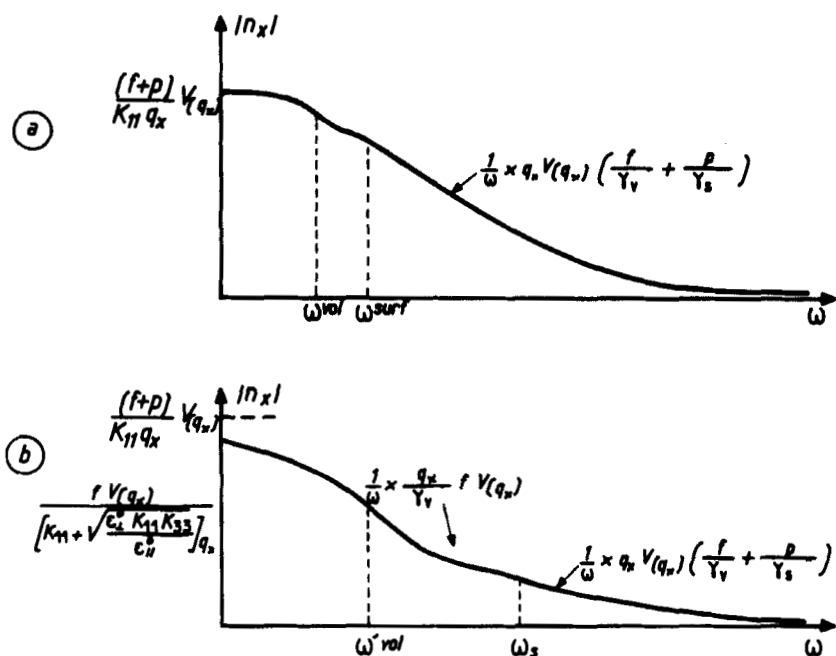$$\delta n_x \simeq \frac{q_x V}{2Gj\omega}\left(\frac{f}{\gamma_V} - \frac{p}{\gamma_s}\right) \quad \text{(II.12)}$$

FIGURE 4 Typical frequency dependence of the induced tilt angle δn_x: (a) weak anchoring conditions ($A \ll K_{33}q_x$): there are two characteristic frequencies in this limit: $\omega^{vol}/2\Pi \simeq K_{11}q_x^2/2\Pi\gamma_v$ and $\omega_s/2\Pi \simeq K_{11}q_x^2/2\Pi\gamma_s$, but volume and surface effects are always mixed. (b) strong anchoring ($A \gg K_{33}q_x$): for $Kq^2/\gamma \ll \omega \ll A^2/K_{33}\gamma$ a viscous regime exists which involves only volume terms. At frequencies higher than $A^2/K_{33}\gamma$ one winds up in the weak anchoring limit, with a mixing of surface and volume terms.

In which:

$$\gamma_V = \cfrac{\gamma_1}{1 + \left((\lambda - 1)\gamma_1 \cfrac{(\lambda - 1)(1 - \sqrt{(2 - \alpha)(\varepsilon_\perp^0/\varepsilon_\parallel^0)} + 2\lambda(\varepsilon_\perp^0/\varepsilon_\parallel^0) + (\lambda + 1)(\varepsilon_\perp^0/\varepsilon_\parallel^0)(\varepsilon_\perp^0/\varepsilon_\parallel^0 - \sqrt{(2 - \alpha)(\varepsilon_\perp^0/\varepsilon_\parallel^0)})}{4v_3(1 + \alpha(\varepsilon_\perp^0/\varepsilon_\parallel^0) + (\varepsilon_\perp^0/\varepsilon_\parallel^0)^2)} \right)}$$

$$\gamma_s^{-1} = \gamma_1^{-1} + \frac{(\lambda + 1)(\lambda + 3)}{4v_3}$$

The indices V and S stand respectively for volume and surface). In the case of MBBA, for which $\lambda \simeq 1$ and $v_3 \simeq (\gamma_1/3)$,[11] $\gamma_V \simeq \gamma_1$ and $\gamma_s \simeq \gamma_1/7$.

—Strong Anchoring: ($q_x \ll q_\omega \ll q_s$)

$$\delta n_x \simeq \frac{q_x V}{2Gj\omega} \frac{f}{\gamma_V} \tag{II.13}$$

Comparison with Eq. II.12 shows that the volume term has exactly the same expression in both strong and weak anchoring limits. Increasing the frequency to meet $q_\omega \gg q_s$ simply adds the term p/γ_s to Eq. II.13. This should in fact provide a way of measuring the anchoring strength (through the knowledge of $\omega_s = A^2/K_{33}\gamma_1$) and the surface polarization, from the increment in the flexoelectric signal.

Eventually, we will keep in mind that strong anchoring conditions are best suited for an experimental study of flexoelectricity, with interdigital electrodes; furthermore if one wants to be able to use simple formulae the optical geometrical conditions should be such that $\delta n_x(q_x, q_z \simeq 0)$ is observed. Last but not least, the most accurate calculations have been performed in the high frequency regime, which will be the best suited domain where to perform experiments, provided one knows the complete set of Leslie or Harvard viscosities (note that, as a result of a rigorous satisfaction of the boundary conditions on the velocity field, the high frequency results Eqs. II.12 and II.13 differ in a non-trivial way from those given in Ref. 8. However, in the absence of surface polarization, the difference is less important.

III   EXPERIMENTAL RESULTS

I   Set up

The scheme of the experiment is displayed on Figure 5. The light source (L) is provided by a Spectra Physics $124AH_e$-N_e laser attenuated down from 6 mW to 60 μW depending on the studied samples. The incident beam may be focussed in any selected plane (electrodes, photocathode, pinhole) by means of Oriel 1522 spatial filter (SF) (in the typical experimental geometry the focussing is achieved in the pinhole plane). Optical detection is imparted to a "La Radiotechnique XP 1116" photomultiplier tube (PM) loaded on a 500 kΩ, 1 kΩ or 50 Ω resistor (depending on the desired frequency bandwidth. A Hewlett–Packard 5082-4207 pin photodiode (P.D.) allows one to check the stability of the incident beam.

The sample is homeotropically aligned by coating the electrodes and coverslide surfaces with hexadecyltrimethylammonium bromide (HTAB), and placed in a home-made oven, the temperature of which is controlled within 10^{-2} °K accuracy. In typical experimental conditions, a sinusoidal voltage (frequency $\omega/2\Pi$) is applied on the electrodes, the amplitude and frequency of which can range from 10^{-2} to 10 V and 2 Hz to 200 kHz, respectively. In that case, the flexoelectric signal is modulated at the same frequency (heterodyning conditions) or at twice this frequency (homodyning
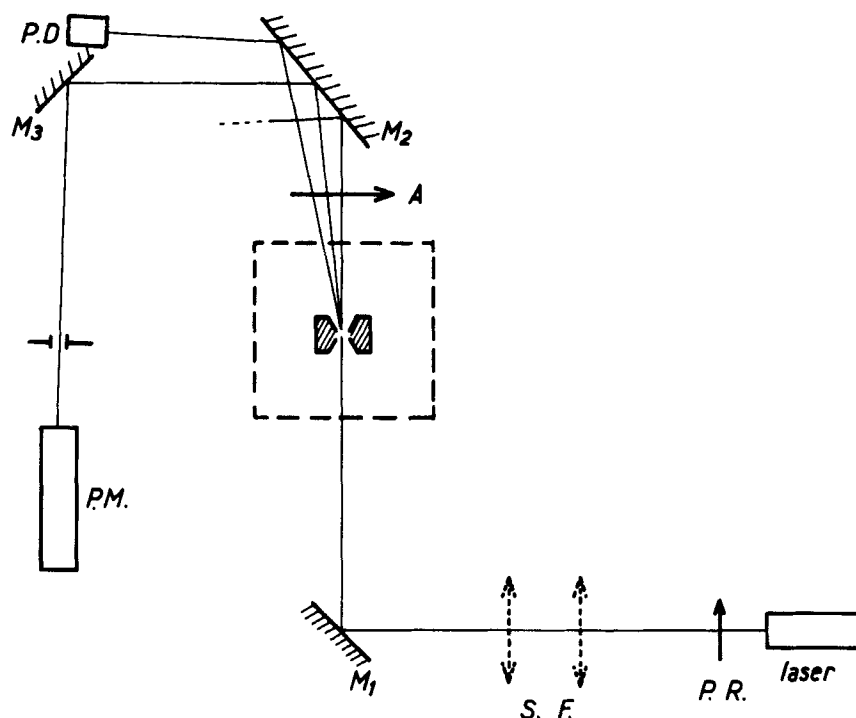
FIGURE 5   Block diagram of the experiment: P.R. polarization rotator, S.F. spatial filter, M_1, M_2, M_3 mirrors, A analyser: P.D. photodiode, P.M. photomultiplier tube. The volume defined by the dotted line represents a thermoregulated oven in the center of which the sample is held.

conditions), which allow in both cases a synchronous detection (PAR 124A lock-in Amplifier) to be used. All experiments begin with the linearity tests, in order to define the voltage that one can safely apply on the electrodes without being perturbed by non-linear effects. Indeed the angular and the frequency selections of the scattered light do not warranty by themselves that one is really dealing with a linear coupling of the electric field with the sample (for instance distortion like $\delta n(q_x, \omega) \alpha \Delta \varepsilon(q_x, \omega) \Phi(q_x, \omega) \Phi(-q_z, -\omega)$, would also give light scattering in the same direction and at the same frequency). Thus checking the proportionality of the scattered amplitude *versus* voltage is a crucial test to make sure that one is dealing with the desired phenomenon. Practically we found that the upper limit at which linearity is found, depends on the dielectric anisotropy value (of the order of a few volts for non or weakly dipolar molecules, and less in the case of the cyano compounds).

The conditions defined in the second section were met with the following orders of magnitude:

$$\begin{cases} D = 500 \ \mu m \\ \lambda_e = \ \ 5 \ \mu m \end{cases} \qquad q_x = \frac{2\Pi}{\lambda_e}$$

$-q_z \ll q_x$: is obtained by using an incident wave vector k_0 normal to the plane of the electrodes (this corresponds to $q_z q_x \simeq q_x/k_0 \simeq 7.4 \ 10^{-2}$ which is not very small, but since the first correction goes as $(q_z/q_x)^2$, one can use with an accuracy better than 1% the formulae derived in the second section). Furthermore, under those conditions, both incident and scattered waves have an extraordinary polarization and the relevant formula of Ref. 8 reduces to:
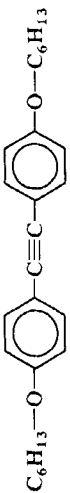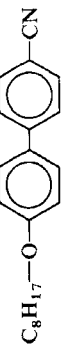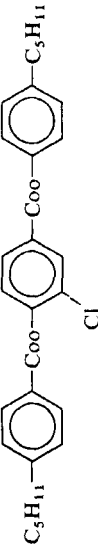
$$\frac{E_s}{E_i} = \frac{(\varepsilon_{\parallel} - \varepsilon_{\perp})}{\varepsilon_{\parallel}} q_x \ \delta n_x(q_x, q_z) \qquad \text{(III.1)}$$

In this relation E_s and E_i are the amplitude of the scattered and incident waves (out of the sample) and $\varepsilon_{\parallel} - \varepsilon_{\perp} = n_e^2 - n_0^2$ the dielectric anisotropy at the optical frequency of the incident laser radiation. $\varepsilon_{\parallel} = n_e^2$ and $\varepsilon_{\perp} = n_0^2$ are the dielectric constants $\parallel$ and $\perp$ to the optical axis. $(n_e - n_0)$ is known to be proportional to the angular order parameter S.[16] Thus the scattered amplitude is essentially a measure of the product $S \ \delta n_x$ (the neglect of the temperature dependence of $(n_e + n_0)/n_e^2$ leads to at most a 6% systematic error; any time enough data were available, the correction has been performed, otherwise it has been neglected (3 PBClB, symmetric tolan).

II Compounds choice

As already mentioned in the first section, we have chosen compounds ranging from symmetric molecules, to strongly dipolar ones (Table I). This follows from the hope that, as is the case for the diamagnetic anisotropy (or the optical frequency dielectric anisotropy) the quadrupolar contribution to f should be of roughly an equal order of magnitude for all these molecules (and essentially governed by the rigid part) whereas Meyer's contribution should range from zero for the symmetric compound to values comparable to the quadrupolar part in the case of molecules with strong dipoles. Hence the flexoelectric coefficient temperature dependence should switch from a pure S dependence in the first case, to a $S + \beta S^2$ in the second. We assume that the flexoelectric activity resulting from induced dipoles is much smaller than any other one. (This hypothesis is born out by our experiments, since the temperature dependence of f for the symmetric pp'hexyloxytolan is essentially proportional to S.

TABLE I

	Formula	Thermotropism	Characteristics
p,p′-dihexyloxytolan "symmetric tolan"	C_6H_{13}—O—⬡—C≡C—⬡—O—C_6H_{13}	K —96.5°C— N —105°C— I	symmetric
p,p′-methoxybenzilidenebutyl-aniline "MBBA"	C_4H_9—⬡—N=CH—⬡—O—CH_3	K —19°C— N —47°C— I	dipolar
p,p′-octyloxycyanobiphenyl "8OCB"	C_8H_{17}—O—⬡—⬡—CN	K —54.5°C— S_A —67°C— N —80°C— I	strongly dipolar
4,n-pentylphenyl,(pentyl-benzoyloxy)-3-chlorobenzoate "3 PBCLB"	C_5H_{11}—⬡—Coo—⬡(Cl)—Coo—⬡—C_5H_{11}	K —23°C— N —124°C— I	low relaxation frequency of longitudinal dipoles 7.14

274

III   Differentiation of volume and surface effects; anchoring conditions

In the theoretical section we have anticipated that the main effect of the charge motion was to screen out the electric field, the metallic pattern of the electrodes being coated with a silicon oxide layer. This can be evidenced either with a sinusoidal voltage at very low frequency ($v \sim 1\,\text{Hz}$ with MBBA) or more clearly by using square waves of longer duration. In all the experiments that we have performed, if one maintains a constant potential on the electrodes, the flexoelectric signal dies away after a characteristic time of a few seconds for room temperature nematics. Figure 2 exhibits the decay of the flexoelectric signal in a typical experiment with MBBA. Three points can be made from such an observation:

—First, the field is indeed screened out in the volume when charges have time to move.

—Second, the signal arises most likely from volume coupling, since one does not expect the screening to be efficient near the glass-liquid crystal interface. These two points were already recognized in Ref. 8. This leaves two possibilities open: either as wanted, strong anchoring conditions are satisfied, or if weak anchoring prevails then $p \ll f$.

—Third, and this hold for MBBA only (presumably with all Schiff bases for experiments on CBOOA lead to the same conclusion); there hardly exists an elastic regime in which charges do not yet have time to move (eg: Figure 2a). Fortunately, more stable compounds do exhibit this elastic regime.

One has then to find a way of estimating the strength of the anchoring energy. This can be achieved only if we have enough information concerning the viscoelastic properties of the studied compounds. This is the case with MBBA and 8OCB. Figure 6 represents the frequency dependence of the flexoelectric signal (scattered amplitude) for MBBA at 23.7°C. One can remark again that one never reaches a genuine elastic regime, but one can still estimate a viscoelastic relaxation frequency by taking explicitly account of the screening effect in the fitting procedure. One finds:

$$v = 27 \pm 5\,\text{Hz}$$

The relatively large uncertainty is precisely due to the screening effect.

This is however enough information to be able to decide whether or not, one has been able to realize strong anchoring conditions: indeed from formulae II.7, 8, 12 and 13 and from the known parameter values [17,18,19,20] ($\gamma_1 \simeq 1$ poise $\gamma_v \simeq \gamma_1 \gamma_s \simeq \gamma_1/7$, $K_{11} \simeq 6 \cdot 10^{-7}$ dyne, $K_{33} \simeq 8 \cdot 10^{-7}$ dyne, $\varepsilon_\perp^0 \simeq 5.3$, $\varepsilon_\parallel^0 \simeq 4.7$ and $q_x = 1.25 \cdot 10^4$ cm^{-1}) one calculates:

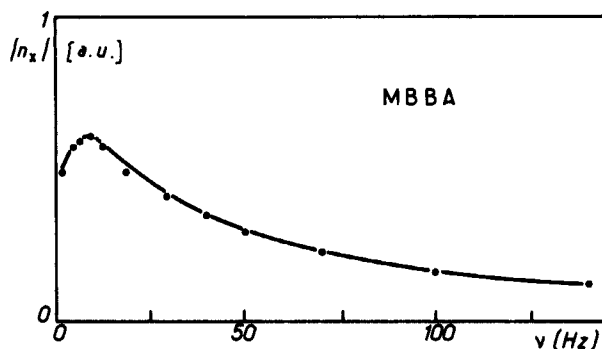$$\text{strong anchoring} \quad v_r = 33 \pm 4\,\text{Hz}$$

FIGURE 6 Flexoelectric signal (scattered amplitude) versus frequency (MBBA, $T = 23.7°C$, $V = 0.5\,V_p$, $\lambda_e = 5\,\mu m$. The solid line is a fit including the screening effect:

$$\delta n_x \propto ((1 + (2.5/\nu)^2)\,(1 + (\nu/27)^2))^{-1/2}$$

weak anchoring $\quad \nu_{vol} = 15 \pm 2\,Hz$

$$\nu_{surf} = 105 \pm 15\,Hz$$

These figures show that the strong anchoring hypothesis is the best suited to explain our results. This is indeed what we wanted to achieve by coating the surfaces with HTAB. Furthermore, we have stressed in the first section that a study of the frequency dependence of the signal should allow to estimate the anchoring strength, since at sufficiently high frequency one should always wind up in the weak boundary condition limit. Such a cross-over, would be best revealed by the plot of the product of the scattered amplitude by the frequency, as a function of frequency. The results concerning MBBA (Figure 7) show that if p is to be considered of comparable magnitude to f (which is suggested by the remarks of Ref. 14) then necessarily:

$$\frac{A^2}{K_{33}\gamma_1} > 2\Pi \cdot 10^5 \qquad A > 0.8\ erg\ cm^{-2}$$

(we take 100 kHz as the upper limit, although we could measure signals up to several megahertz, because above this value our accuracy drops from: 2% to $\pm 10\%$ around 1 MHz). If one does not want to make any assumption on p, one can still assert, from the low frequency study: $A \gg K_{33}q_x$, that is:

$$A \gg 10^{-2}\ erg\ cm^{-2}\ (K_{33} = 8 \cdot 10^{-7}\ dyne\ q_x = 1.25 \cdot 10^4\ cm^{-1})$$

In the case of 8OCB, an indirect argument is provided by the results of the temperature dependence of the low frequency temperature signal (Figure 8). The scattered amplitude is proportional to (fSK^{-1}), with $K = K_{11}$ for weak anchoring and $K = K_{11} + ((\varepsilon_\perp^0/\varepsilon_\parallel^0)K_{11}K_{33})^{1/2}$ for strong anchoring. It is known that K_{33} diverges near the $N-S_A$ transition while K_{11} does not;[22] thus the abrupt decrease of the scattered amplitude near this transition can
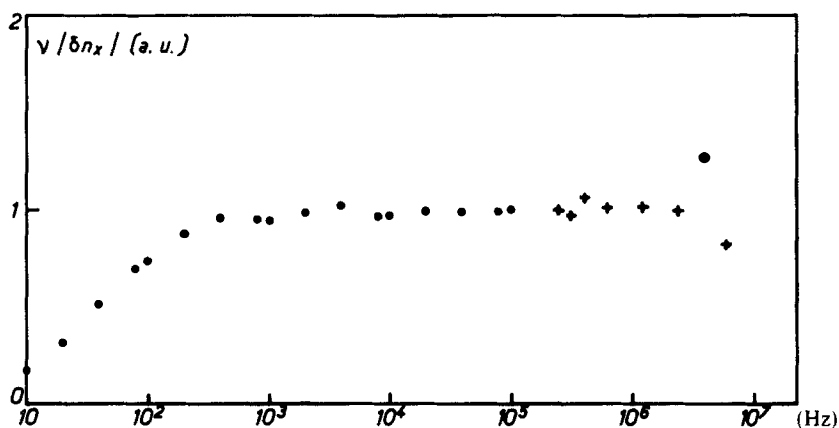
FIGURE 7 Frequency dependence of the flexoelectric signal: $v \cdot |\delta n_x| = f(v)$ (MBBA, $T = 28°C$, $\lambda_e = 5 \mu m$, $V = 0.5 V_p$). Dots and crosses refer to different detection schemes $\{^{10,21}\}$. Note the remarkable constancy of $f(v)$, revealing the $1/v$ dependence of δn_x over more than four frequency decades.

only be understood if rigid boundary conditions prevail. Hence, for 8OCB too:

$$A \gg 10^{-2} \text{ erg cm}^{-2}$$

These conclusions are opposite to the one reached in[8] for a p-butoxy-benzal-p-β-methylbutylaniline (BBMBA)–HTAB–glass interface. We believe that for this last compound, there were not enough data available to
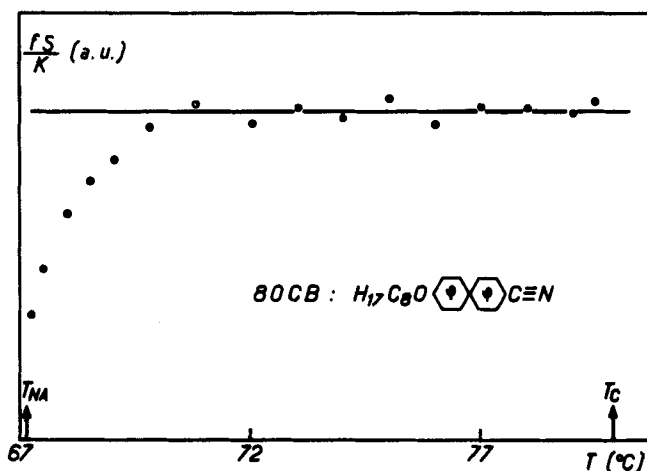

FIGURE 8 8OCB: $V = 0.5 V_p$ $\lambda_e = 5 \mu m$, $v = 45$ Hz. Square root of the homodyne signal versus temperature in the elastic regime. The solid line stresses the constancy of this signal above 70°C.

allow for a definitive conclusion, although it is quite possible that boundary conditions change drastically from one compound to another.

IV   Dipolar versus quadrupolar flexoelectricity

We have stressed in the introduction that the knowledge of the thermal dependence of f should allow us to have an estimate of the relative importance of the quadrupolar and Meyer's flexoelectricities. Indeed, the formula II.9 of Ref. 2 can be written:

$$f = f^M + f^Q$$

with

$$f^M = \alpha_{\parallel} K_{11}(\varepsilon_{\parallel}^0 - \varepsilon_{\parallel}^1) + \alpha_{\perp} K_{33}(\varepsilon_{\perp}^0 - \varepsilon_{\perp}^1) \tag{III.2}$$

$$f^Q = \tfrac{1}{3}\Theta_a(L_{\parallel} + L_{\perp})$$

α is a coefficient characterizing the asymmetry of the molecule ($\alpha_{\parallel}$ pear-like; $\alpha_{\perp}$ banana-like); ($\varepsilon_{\parallel \perp}^0 - \varepsilon_{\parallel \perp}^1$) is the contribution of the longitudinal (resp: transverse) permanent dipole to the dielectric constant; Θ_a is the macroscopic electric quadrupole. $L_{\parallel \perp}$ is the Lorentz coefficient (resp. parallel and perpendicular to the director). The leading temperature dependence of f^M is given by the Frank elastic constant, which is known to be essentially proportional to S. In fact the Lorentz factor may include a small contribution proportional to S (due to its anisotropic part) although it is known to be essentially temperature independent.[16] Then complete association of the S^2 dependent term with the dipolar contribution is thus not quite correct, but is suggested by the fact that some results involve almost no S^2 term indicating that the Lorentz correction temperature dependence is indeed small.

We have plotted on the Figures 8, 9 and 10, the results concerning the 8OCB, the symmetric tolan, and MBBA. In the first two cases the measurements were performed in the elastic regime; the ratio fS/K is directly accessible to the experiment in this regime, and is a constant if $f \alpha S$. This is indeed the case for these two compounds (except in the pretransition region of 8OCB near T_{NA}, where K_{33} departs from its S^2 dependence and diverges). The existence of flexoelectricity is thus demonstrated for the first time with a symmetric compound, and the S dependence shows its quadrupolar origin. It may at first sight be surprising that one obtains the same result with 8OCB. However, X-Ray measurements show the formation of pairs of molecules with antiparallel dipoles[23,24,25] which certainly decrease the dipolar contribution, and lead to the definition of an effective molecular quadrupole.[2,21] This result provides thus a confirmation of the formation of the dipole pairs. In the case of MBBA, the measurements were performed in the viscous regime since, as we already noticed, the elastic regime is not fully accessible and enough
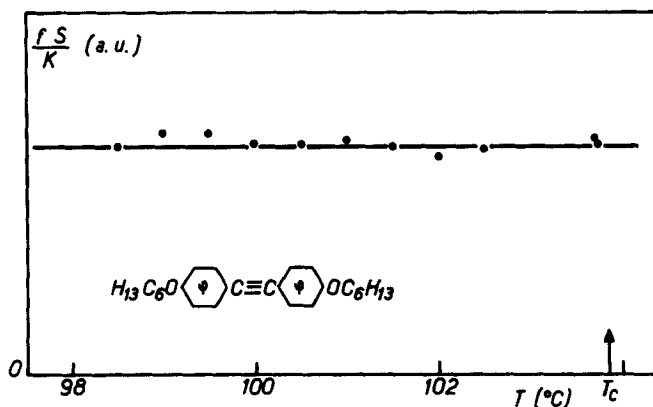
FIGURE 9 Symmetric tolan. ($V = 0.5\, V_p$, $\lambda_e = 25\,\mu m$, $v = 35$ Hz). Square root of the homodyne signal versus temperature in the elastic regime. The solid line stresses the constancy of this signal in the whole nematic range.

information is available to exploit the high frequency data. In that case the ratio fS/γ_1 is provided by the experiment. $\gamma_1(T)$ and $S(T)$ are known from Refs. 19 and 26.

A mean least square fit gives: $f \propto S + 0.3S^2$; hence, since S is typically of the order of 0.5, the dipolar part of f amounts at most to 15% of the total value. This result can be compared with the one obtained from the frequency
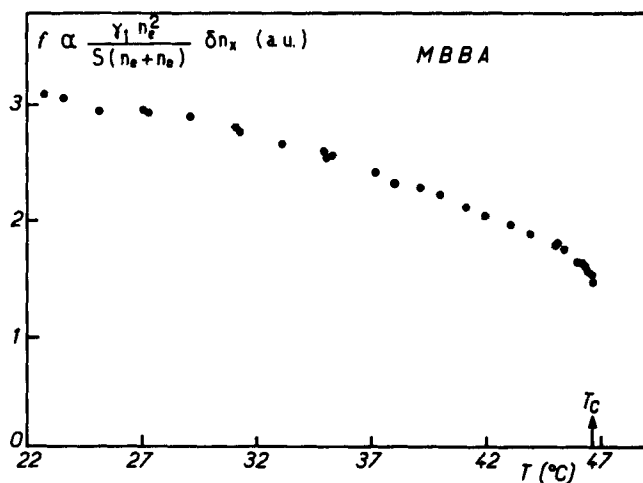

FIGURE 10 MBBA ($V = 0.5\, V_p$, $\lambda_e = 5\,\mu m$, $v = 235$ Hz). Square root of the homodyne signal in the viscous regime multiplied by:

$$\gamma_1/S\,(n_e^2/n_e + n_o)$$

Note the temperature dependence characteristic of the anisotropic part of almost any kind of second rank tensor in the nematic phase.

dependence reported in Figure 7: since the longitudinal dipoles relaxation frequency lies in the Megahertz domain (1.1 MHz at room temperature,[20] if dipolar flexoelectricity was to show up one should be able to evidence a relaxational behavior in Figure 7. The relative inaccuracy of the experiment in this frequency range leads us to the conclusion: $f^M < 20\% f^{10}$ in agreement with our temperature dependence result, and also early estimates of f^M.[1,3,5]

At last, let us briefly recall the result obtained with 3PBClB. We stressed in the introduction that this compound has been chosen for the very low relaxation frequency of its longitudinal dipoles; further interesting features were its ($\varepsilon_\parallel^0 - \varepsilon_\parallel^1$) value (five times larger than that of MBBA) and the lack of tendency to build up pairs of antiparallel dipoles. Figure 11, indeed, reveals a clear relaxational behavior, at the frequency expected from dielectric experiments.[27] A cross over from rigid to weak boundary conditions would in principle lead to the same observation. However, the temperature dependence of the relaxation frequency is typical of the dipolar relaxation. It would have been interesting to investigate the whole 3PBClB nematic range, but we have been unable to warranty a reliable alignment of the sample at temperatures higher than 60°C (as a result the frequency dependence of the signal bares no resemblance with the one exhibited in Figure 11, and depends on the aging of the sample, which indeed was not the case at lower temperatures). In any case, we could estimate:

$$f_\parallel^M \simeq 30\%(f^M + f^Q) \text{ for } T < 60°C$$

V   Estimate of the coefficients

As it is obvious from the theoretical section, we can only give reasonably accurate estimates of f in the case of well-known compounds namely MBBA and 8OCB. Since both experiments correspond to rigid boundary conditions, with the use of Eqs. II.13 and III.1, one obtains in the viscous regime:

$$f = \frac{2G\gamma_v\omega}{V} \frac{\varepsilon_\parallel}{(\varepsilon_\parallel - \varepsilon_\perp)q_x^2} \left|\frac{E^s}{E^i}\right| \qquad (III.3)$$

For MBBA, at 35°C one finds: $|E_s/E^i| \simeq (1.08)\cdot 10^{-2}$ for $V = 1$ Volt (peak), $\omega/2\pi = 235$ Hz and $q_x = 1.25\cdot 10^4 \text{cm}^{-1}$. With $\varepsilon_\perp \simeq 2.39$, $\varepsilon_\parallel \simeq 3.01$;[28] $\gamma_v = 0.65$[17,18,19] thus:

$$f_{\text{MBBA}} \simeq (7.1 \pm 1.4)\cdot 10^{-4} \text{ esu}$$

The accuracy of the measurement of E_s/E^i is of the order of 2%, additional parameters such as γ_v, $\varepsilon_\parallel$, $\varepsilon_\perp$ and so on introduce an uncertainty of about 10%, but since, as discussed in Ref. 8, higher Fourier components
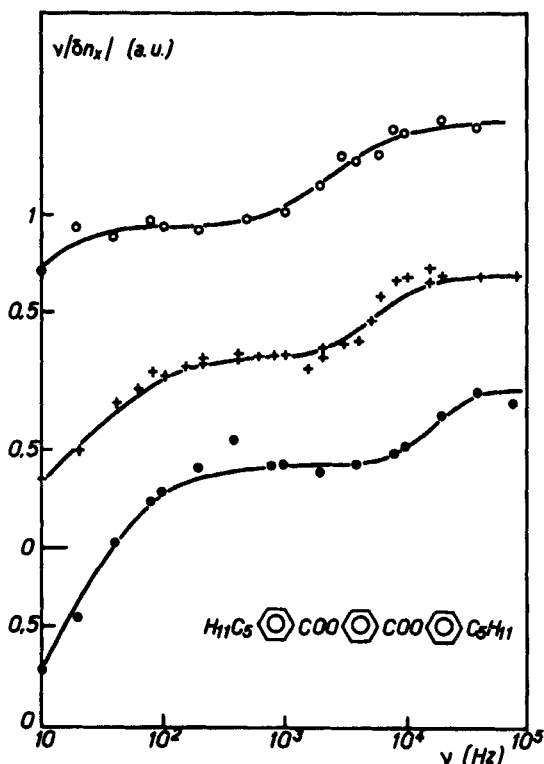
FIGURE 11 3 PBCLB ($V = 0.1\ V_p$, $\lambda_c = 5\ \mu$m). Heterodyne signal A (v) multiplied by the frequency versus frequency, at three different temperatures (0: $T = 28°C$, $+$: $T = 41.5°C$; $.$: $T = 57.6°C$; for the sake of clarity the curves have been vertically shifted). Clearly visible are:— $v < 100$ Hz: the viscoelastic relaxation frequency $v_v - v$ on the KHz range, the dipole relaxation frequency v_r. The solid line is a fit according to the law:

$$ f \propto v|A(v)| \propto \left(\frac{v\left(\{(f - f_\|^M\} + \dfrac{f_\|^M}{1 + j\,v/v_r} \right)}{1 + j\dfrac{v}{v_v}} \right) $$

($T = 28°C$: $v_r = 3$ KHz; $T = 41.5°C$: $v_r = 5.5$ KHz; $T = 57.6°C$: $v_r = 14$ KHz)

($q_x = n(2\pi/\lambda e)$) may contribute to a small fraction of the scattered intensity (no more than 6%), we estimate the total uncertainty to be of the order of 15% to 20%.

This result compares well with the raw data obtained by the Sofia group ($f \simeq 8 \cdot 10^{-4}$ esu),[29] but only an order of magnitude wise with their corrected value ($f \simeq 3 \cdot 10^{-4}$ esu).

For 8OCB, at 73°C one finds:

$$\frac{E_s}{E^i} \simeq (7.3)\ 10^{-3} \quad \text{with} \quad \frac{\omega}{2\pi} = 660\ \text{Hz}, \qquad V = 1\ V$$

and

$$q_x = 1.25\ 10^4\ \text{cm}^{-1}$$

Estimating: $\gamma_1 \simeq 0.3$ poise[30,31] $\varepsilon_{\parallel} \simeq 2.85\varepsilon_{\perp} \simeq 2.25$[32]

$$f_{8OCB} \simeq (6.4 \pm 1.5) \cdot 10^{-4}\ \text{esu}.$$

Note that although the dipolar character of 8OCB is strongly different than that of MBBA, the flexoelectric coefficient values are very similar. This is quite understandable in a quadrupolar picture, but would be hard to understand in a purely dipolar model.

In the case of the other compounds, we can only give an estimate of the ratio f/K:

—symmetric tolan: $f/K \simeq 8 \cdot 10^2$ esu at 99.3°C
— 3PBClB $\qquad f/K \simeq (2.8) \cdot 10^2$ esu at 48.9°C

The figures are in agreement with flexeoelectric coefficients of a few 10^{-4} esu, if we assume elastic constants in the 10^{-6} dyne range.

Let us remark that the MBBA and 8OCB flexoelectric coefficient values are roughly twice the one found in Ref. 8 for BBMBA, the calculation had been performed under the assumption of free boundary conditions. The comparison with our current data shows that if rigid boundary conditions were more appropriate this would bring the BBMBA value in the same range as the others.

At last let us point out that although it is possible to measure the difference $(f_{\parallel} - f_{\perp})$[33,34,35] such an attempt has not been performed since both the dipolar and the quadrupolar mechanisms predict a S^2 dependence for that coefficient.

IV CONCLUSION

We have obtained through this experimental study a number of results which point toward an understanding of flexoelectricity based mainly on the quadrupolar interpretation:

—The phenomenon is shown to exist with a symmetric molecule, for which the coefficient $f = f_{\parallel} + f_{\perp}$ exhibits a S (rather than S^2) dependence.

—The observed temperature dependences also show a leading S behavior for f, in the case of other compounds.

—The estimated order of magnitudes of f lies in the same range for all compounds, although the dipolar character of the molecules is drastically different from one compound to the other.

In particular our results with 8OCB, confirm the known fact that these molecules form pairs with antiparallel dipoles. We have been able to find a compound, which clearly exhibits Meyer's mechanism. For having a chance of performing such an observation one has to choose a molecule with a relatively strong longitudinal dipole $(\varepsilon_{\parallel}^{1} - \varepsilon_{\parallel}^{0})$ "large", but with some steric hindrance that it will not be strong enough to build up pairs.

Acknowledgments

References

1. R. B. Meyer, *Phys. Rev. Lett.*, **22**, 918 (1969).
2. J. Prost and J. P. Marcerou, *J. Phys.*, **38**, 315 (1977).
3. W. Helfrich, *Z. Naturforsch*, **26a**, 833 (1971).
4. W. Helfrich, *Mol. Cryst.*, **26**, 1 (1974).
5. Derzhanski and A. G. Petrov, *Phys. Lett.*, **36A**, 483 (1971).
6. H. Gruler, *J. Chem. Phys.*, **61**, 5408 (1974).
7. J. P. Straley, *Phys. Rev.*, **A14** (1976), 1835 (1976).
8. J. Prost and P. S. Pershan, *J. Appl. Phys.*, **47**, 6 (1976).
9. J. P. Marcerou and J. Prost, *Phys. Lett.*, **66A**, 218 (1978).
10. J. P. Marcerou and J. Prost, *Ann. de Phys.*, **3**, 269 (1978).
11. P. G. de Gennes, *The Physics of Liquid Crystals*, Clarendon Oxford Press (1974).
12. P. C. Martin, O. Parodi, and P. S. Pershan, *Phys. Rev.*, **A6**, 2401 (1972).
13. F. M. Leslie, *Arch. Rat. Mech. Anal.*, **28**, 265 (1968).
14. A. G. Petrov and A. Derzhanski, *Mol. Cryst. Liq. Cryst., (Lett.)*, **41**, 41 (1977).
15. J. D. Parsons, *Phys. Rev. Lett.*, **41** (1978), 877 (1978).
16. S. Jen, N. Clark, P. S. Pershan, and E. B. Priestly, *Phys. Rev. Lett.*, **31**, 1552 (1973). See also: N. V. Madhusudana, R. Shashidar, and Chandrasekhar, *Mol. Cryst. Liq. Cryst.*, **13** 61 (1971).
17. C. Gahwiller, *Phys. Lett.*, **36A**, 311 (1971).
18. I. Haller and H. Huggins, IBM Research R.C., 1972, 3772.
19. J. Prost and H. Gasparoux, *Phys. Lett.*, **36A**, 245, (1971).
20. F. Rondelez and A. Mircea-Roussel, *Mol. Cryst. Liq. Cryst.*, **28**, 173 (1973).
21. J. R. Marcerou, Thèse de spécialité—Bordeaux (1978). N° d'ordre 1412.
22. P. G. Gennes, *Sol. St. Comm.*, **11**, 1615 (1972). In the particular case of 8OCB the regular behavior of K_{11} has been evidenced by H. Birecki, R. Schaetzing, F. Rondelez, J. D. Litster, *Phys. Rev. Lett*, **36**, 1376 (1976) on the smectic side of the N-A transition, and on the nematic side by: R. J. Birgeneau, F. Garcia-Golding, M. Kaplan, J. D. Litster, C. R. Safinya *7th Int. Liq. Cryst. Conf. Bordeaux*, (1978).
23. A. J. Leadbetter, R. M. Richardson, and C. N. Colling, *J. Phys. Coll.*, **CI**, **36**, C1. 37 (1975).
24. J. E. Lydon and C. J. Coakley, *J. Phys. Coll.*, CI, **36**, CI. 45 (1975).

25. P. E. Cladis, R. K. Bogardus, W. B. Daniels, and G. N. Taylor, *Phys. Rev. Lett.*, **39**, 720 (1977).
26. J. Prost, Thèse Bordeaux N° 392 (1973).
27. R. T. Klingbiel, D. D. Genova, and H. K. Bucher, *Mol. Cryst. Liq. Cryst.*, **27**, 1 (1974).
28. M. Brunet-Germain, *C. R. Acad. Sci.*, **271**, 1075 (1970). See also—B. Martin, Thèse de spécialité Bordeaux N° 261 (1977).
29. A. I. Derzhanski and M. Mitov, *C. R. Acad. Sci. Bulg.*, **28**, 1331 (1975).
30. L. Leger and A. Martinet, *J. Phys. Coll.*, C3 **37**, C3-89 (1976).
31. F. Hardouin, Thèse Bordeaux N° 559 (1978).
32. M. Delaye, Thèse Orsay (1978).
33. J. P. Bobylev and S. A. Pikin, *Zh. Eksp. Theor. Fiz.*, **72**, 369 (1977).
34. M. I. Barnik, L. M. Blinov, A. N. Trufanov, and B. A. Unmanski, *J. de Phys.*, **39**, 417 (1978).
35. J. Prost, *J. de Phys.*, **39**, 639 (1978).